Mass effects of light ion swarms in ac electric fields

R. D. White*
School of Mathematical and Physical Science, James Cook University, Cairns QLD 4870, Australia
(Received 3 June 2001; published 24 October 2001)

Transport properties of light ions in gases in ac electric fields are investigated by solving the time-dependent Boltzmann's equation. We focus on the way in which transport properties including diffusion are influenced by the ion-neutral mass ratio as well as the field frequency. Calculations of transient relaxation phenomena in step-function fields are performed as an aid to understanding the complex temporal profiles of ion transport coefficients in ac electric fields.

DOI: 10.1103/PhysRevE.64.056409 PACS number(s): 51.10.+y, 52.25.Fi, 52.20.−j, 52.80.Pi

I. INTRODUCTION

The study of charged-particle transport in gases under the influence of ac electric fields has application in diverse areas ranging from lasers and plasma discharges [1] through to muon catalyzed fusion [2]. In recent times however, there has been much focus on gaseous electronics applications. It is generally acknowledged that future optimization of industrial applications involving radiofrequency/microwave gaseous discharges requires a detailed knowledge of the transport theory of charged particles in gases under the influence of oscillating electric fields [1,3]. In contrast to the electron component of the plasma discharge models, the kinetic theory of the ion component has generally been neglected, preferring other treatments (e.g., fluid models, Monte Carlo techniques) and often severe approximations. The need for a systematic investigation of the kinetic theory of ion component ac discharges is high and represents the principal aim of this work. As a first step toward this goal, we address those charged particles in the bulk of a weakly ionized plasma far away from the electrodes. Here the electric field is approximately homogeneous in space, though periodic in time. This is commonly referred to as the swarm problem.

The majority of the literature for charged-particle swarms in ac electric fields, including the pioneering works of Holstein [4], Margenau and Hartman [5], and Brown and coworker [6], has focused on electron swarms (see, for example, works of Winkler and co-workers [7–11], Makabe and co-workers [12–16], Ferreira and co-workers [17–20], Petrovic and co-workers [21–24], as well as by us [25,26,27,28,29]). This path of investigation may in part be a result of the mathematical simplifications, which result from the smallness of the electron to neutral mass ratio. These simplifications were employed by foundation workers in the dc field swarms (e.g., the ''two-term'' approximation and the reduction of the Boltzmann collision operator [30] to the Davydov differential form [31]) and were adopted by the pioneer workers in ac electric field swarms [4–6]. Further assumptions on the temporal variation of certain Legendre components (e.g., the quasistationary [4], effective field approximations [6,17,32], low-order Fourier series truncations [5,12,13,20]) facilitated analytic solution and these assumptions have since become embedded in much of the literature on electron kinetics in rf discharge modeling [32,33]. The restrictions on the gas types and field frequencies associated with such approximations/theories are now well known. Recent advances in the kinetic theory of ac electron swarms have overcome many of these restrictions [14–16,25,27,28]. Extensions have also been made to consider spatially inhomogeneous electron swarms in ac electric fields yielding the important phenomena of anomalous anisotropic diffusion [16,25,27,28]. Striking effects on transport coefficients in ac electric fields associated with nonconservative collisional processes have also been observed [22,29].

In contrast to the extensive literature on ac electron swarms, the kinetic theory of ion swarms in ac electric fields has received little investigation in comparison. In spite of the well-known literature on dc ion swarms (see, e.g., Ref. [34] and references therein), Boltzmann's equation treatments of the ac problem have, in general, been restricted to model collision operators [e.g., the Bhatnager-Gross-Krook (BGK) collision operator for idealized charge transfer collisions [35–37]] and low-order truncation of moment equations [38]. The aim of this paper is to combine the theoretical foundations developed for ac electron swarms [25,27,29] with the extensive mathematical infrastructure developed for dc ion swarms [39–42] to consider the first systematic treatment of ion swarms in ac electric fields.

In Sec. II, we briefly review the time-dependent multiterm solution of Boltzmann's equation. No assumptions are made concerning the following: (1) the number of spherical harmonics required, this is determined solely through predefined accuracy requirements; (2) the temporal dependence of spherical harmonic coefficients, this theory is thus valid for arbitrary field frequencies; (3) spatial uniformity (subject to the existence of a time-dependent hydrodynamic description [29]). In this initial study, for demonstrative purposes we do, however, restrict the form of the interaction to a constant elastic cross section. It is emphasized that the theory and associated code are valid for more realistic cross sections. We restrict our discussion to ion to neutral mass ratios in the range $10^{-4}-0.1$. Higher order mass ratios, though calculable under dc steady state conditions, proved too expensive computationally for *time-dependent* systems. In Sec. III, we present a systematic investigation of the variation of the temporal profiles of the transport coefficients with the applied

*Electronic address: Ronald.White@jcu.edu.au

frequency over the range charged-particle to neutral-particle mass ratios are considered.

II. THEORY

The governing equation describing a swarm of charged particles moving through a background of neutral molecules in a time-dependent electric field $E(t)$ is Boltzmann's equation for the phase-space distribution function $f(\boldsymbol{r},\boldsymbol{c},t)$,

$$\frac{\partial f}{\partial t}+\boldsymbol{c}\cdot\boldsymbol{\nabla} f+\frac{e\boldsymbol{E}(t)}{m}\cdot\frac{\partial f}{\partial \boldsymbol{c}}=-J(f,f_0). \tag{1}$$

Here $\boldsymbol{r}$ and $\boldsymbol{c}$ denote respectively the position and velocity coordinates in phase space while e and m are the charge and mass of the swarm particle, respectively. Swarm conditions are assumed to apply and $J(f,f_0)$ denotes the rate of change of f due to binary particle-conserving collisions of the charged particle with neutral particles whose distribution function f_0 is Maxwellian at a temperature T_0. We employ the original Boltzmann equation collision operator [30] and make no assumptions on the charged-particle to neutral-particle mass ratio in this work.

In a previous paper [29], the theoretical formalism for charged-particle swarms in non-conservative gases in ac fields was developed. This theory was equally valid for both electron or ion swarms, though the paper focused on electron or light ion swarms. In what follows we briefly review the spherical harmonic/Burnett function decomposition (two-temperature theory) of the Boltzmann's equation under time-dependent hydrodynamic conditions. For further details the reader is referred to Refs. [43] (hereafter referred to as I) and [29] (hereafter referred to as II).

(a) Spherical-harmonic expansion. The directional dependence of the phase-space distribution function in velocity space is represented in terms of a spherical harmonic expansion,

$$f(\boldsymbol{r},\boldsymbol{c},t)=\sum_{l=0}^{l_{max}}\sum_{m=-l}^{l} f_m^{(l)}(\boldsymbol{r},c,t)Y_m^{[l]}(\hat{\boldsymbol{c}}), \tag{2}$$

where $\hat{\boldsymbol{c}}$ represents the angles of $\boldsymbol{c}$. The value of l_{max} is incremented until some predefined accuracy criterion is satisfied. This value indicates the deviation of the velocity distribution function from isotropy.

(b) Density gradient expansion. Assuming a time-dependent hydrodynamic regime (the restrictions of which are detailed in Ref. [29]), the spatial dependence is represented by

$$f_m^{(l)}(\boldsymbol{r},c,t)=\sum_{s=0}^{1}\sum_{\lambda=0}^{s} f(lm|s\lambda;c,t)G_m^{(s\lambda)}n(\boldsymbol{r},t), \tag{3}$$

where $G_m^{(s\lambda)}$ is the irreducible gradient operator [44]. Truncation at $s=1$ is sufficient to determine transport coefficients up to and including diffusion under conservative conditions. A higher order truncation is required in the presence in non-conservative collisional processes [29,45].

(c) Sonine polynomial expansion. Finally the speed dependence of the coefficients in Eq. (3) is represented by an expansion about a Maxwellian at an arbitrary *time-dependent* temperature $T_b(t)$, in terms of Sonine polynomials,

$$f(lm|s\lambda;c,t)=w(\alpha(t),c)\sum_{\nu=0}^{\infty} F(\nu lm|s\lambda;\alpha(t),t) \times R_{\nu l}(\alpha(t)c), \tag{4}$$

where

$$R_{\nu l}(\alpha(t)c)=N_{\nu l}\left[\frac{\alpha(t)c}{\sqrt{2}}\right]^l S_{l+1/2}^{(\nu)}\left[\frac{\alpha^2(t)c^2}{2}\right], \tag{5}$$

$$w(\alpha(t),c)=\left[\frac{\alpha^2(t)}{2\pi}\right]^{3/2}\exp\left\{-\frac{\alpha^2(t)c^2}{2}\right\}, \tag{6}$$

$$\alpha^2(t)=\frac{m}{kT_b(t)}, \tag{7}$$

$$N_{\nu l}^2=\frac{2\pi^{3/2}\nu!}{\Gamma(\nu+l+3/2)}, \tag{8}$$

and $S_{l+1/2}^{(\nu)}(\alpha^2(t)c^2/2)$ are Sonine polynomials. The expansions (2) and (4) amount to the two-temperature Burnett function used extensively in dc electron and ion swarms investigations [42,43]. The moments $F(\nu lm|s\lambda;\alpha(t),t)$ satisfy the parity, symmetry, reality, and normalization conditions, Eqs. (5) and (6) of I. The requirement for a time-dependent weight function has been detailed previously [25,29,46]. Briefly, convergence of expansion (4) for a given T_b is satisfied over a limited range of applied fields or equivalent mean energies. When the mean energy falls outside this range, T_b must then be appropriately modified.

Using the orthonormality conditions of the spherical harmonics and modified Sonine polynomials, the following generalization to the time-dependent regime of the hierarchy of kinetic equations, Eqs. (16), (18), and (20), follows:

$$\sum_{\nu'=0}^{\infty}\sum_{l'=0}^{\infty}[\partial_t\delta_{\nu\nu'}\delta_{ll'}+n_0J_{\nu\nu'}^l(\alpha(t))\delta_{ll'}+ia(t)\alpha(t) \times(l'm10|lm)\langle\nu l||K^{[1]}||\nu' l'\rangle]F(\nu' lm|s\lambda;\alpha(t),t) =\overline{X}(\nu lm|s\lambda;\alpha(t),t), \tag{9}$$

$$(\nu,l)=0,1,2,\ldots,(\nu_{max},l_{max}),$$

$$|m|\leqslant\min\{l,\lambda\},$$

$$s+\lambda \text{ is even.}$$

Explicit expressions for the required right-hand side vectors are given in Eq. (16) of I. The reduced matrix elements of the velocity derivative and velocity are given by Eqs. (12a,b) of I, respectively.

The calculation of the collision matrix elements $J_{\nu\nu'}^l$, defined by Eq. (11) of I, for the ''two-temperature'' moment

theory has been developed extensively over the last 20 years and is quite general in its applicability. In particular, we use the Talmi transformation methods of Kumar [41] that allow for separation of mass and interaction effects. We further expand the mass-dependent component in terms of a mass ratio expansion,

$$J^l_{\nu\nu'}=\sum_{s=0}^{\infty}\left(\frac{m}{m+m_0}\right)^s J^l_{\nu\nu'}(s). \tag{10}$$

We truncate this expansion to the number of terms required to achieve a predefined accuracy. A discussion of the calculation of the collision matrix is beyond the scope of this paper and the reader is referred to Ref. [39]. The computation time for calculating the matrix elements of the collision operator increases with increasing mass ratio due to increased number of terms required in Eq. (10) to achieve convergence. Herein lies the origin of our restriction on the mass ratios considered: for time-dependent systems a range of basis temperatures is required and the collision matrix must be evaluated for each T_b.

An implicit finite difference scheme is employed to evaluate the partial time derivatives in Eq. (9). The expression (14) in II is used to relate moments with different basis temperatures at different time steps.

At the nth time step, the transport coefficients of interest are related to the calculated moments via

$$W^n=\frac{i}{\alpha_n}F^n_{\alpha_n}(010|00), \tag{11}$$

$$D^n_L=-\frac{1}{\alpha_n}F^n_{\alpha_n}(010|11), \tag{12}$$

$$D^n_T=-\frac{1}{\alpha_n}F^n_{\alpha_n}(011|11). \tag{13}$$

The spatially homogeneous mean energy $\varepsilon(t)$ and the gradient energy vector $\boldsymbol{\gamma}(t)$ [25,28] defined through a density gradient expansion of the average swarm energy $\boldsymbol{\epsilon}(\mathbf{r},t)$,

$$\boldsymbol{\epsilon}(\mathbf{r},t)=\frac{1}{n(\mathbf{r},t)}\int\frac{1}{2}mc^2 f(\mathbf{r},\mathbf{c},t)d\mathbf{c}=\varepsilon(t)+\boldsymbol{\gamma}(t)\cdot\frac{\nabla n}{n}+\cdots, \tag{14}$$

play pivotal roles in the qualitative understanding of the temporal profiles of the drift and diffusion coefficients. These quantities in a Burnett function basis are given by

$$\varepsilon^n=\frac{3}{2}kT^n_b\left[1-\sqrt{\frac{2}{3}}F^n_{\alpha_n}(100|00)\right], \tag{15}$$

$$\gamma^n=\frac{3}{2}kT^n_b\left[i\sqrt{\frac{2}{3}}F^n_{\alpha_n}(100|11)\right]. \tag{16}$$

In addition, to further explore the anisotropic nature of ion diffusion, we calculate the elements of the (spatially averaged) temperature tensor, the transverse element T_T, and longitudinal element T_L,

$$T^n_T=T^n_b\left[1-\sqrt{\frac{2}{3}}F^n_{\alpha_n}(100|00)+\sqrt{\frac{1}{3}}F^n_{\alpha_n}(020|00)\right], \tag{17}$$

$$T^n_L=T^n_b\left[1-\sqrt{\frac{2}{3}}F^n_{\alpha_n}(100|00)+\sqrt{\frac{1}{3}}F^n_{\alpha_n}(020|00)-\frac{2}{\sqrt{3}}F^n_{\alpha_n}(020|00)-\{F^n_{\alpha_n}(010|00)\}^2\right]. \tag{18}$$

This ends the general theoretical decomposition of the Boltzmann's equation in the time-dependent hydrodynamic regime. For a discussion of the numerical aspects of the solution of the hierarchy (9), the reader is referred to [29,43].

III. RESULTS AND DISCUSSION

The aim of this section is to systematically investigate the effect of varying the charged-particle to neutral-particle mass ratio m/m_0 on the transport properties of charged-particle swarms in ac electric fields of various frequencies. We limit our discussion to a model interaction cross section, preferring instead to isolate the effects of the mass ratio rather than further complicating the effects by introducing real cross sections that generally introduce further complexity. In particular we employ a gas of hard spheres (at a temperature $T_0=293$ K and each with a mass $m_0=4$ amu) with a charged-particle to neutral-particle cross section of 6 Å^2. For simplicity, scattering is assumed isotropic and elastic. These restrictions can easily be relaxed in subsequent studies of more realistic situations. The neutral mass is fixed and the swarm-particle to neutral-particle mass ratio is varied between 10^{-4} and 0.1. We consider a harmonic field of the form $E/n_0=1(\cos\omega t)$ Td, where 1 Td$=1\times10^{-21}$ V m^2. The quantities calculated in the following sections are functions of the reduced angular frequency ω/n_0, where ω is the frequency of the field and n_0 is the neutral number density.

In what follows we briefly investigate general phenomenology of transport coefficients in ac electric fields. These concepts are then employed to investigate the ac profiles of the spatially homogeneous transport properties (drift velocity and mean energy). The effects of spatial gradients are considered in Sec. III D, focusing on the anisotropic nature of diffusion in ion swarms and associated effects, including the anisotropic nature of the temperature tensor and the gradient energy parameter.

A. General phenomenology in ac electric fields

In general it is not possible to obtain the temporal profiles of transport properties in ac electric fields through a simple extrapolation of steady state dc results or arguments. In what follows we discuss traditional qualitative explanations of the temporal profiles of electron swarms in ac fields in Sec. III A 1 and highlight their inability to qualitatively explain certain phenomena. We then outline a scheme by which the detailed structure in the ac profiles can be understood through the use of relaxation profiles. Initially, we restrict

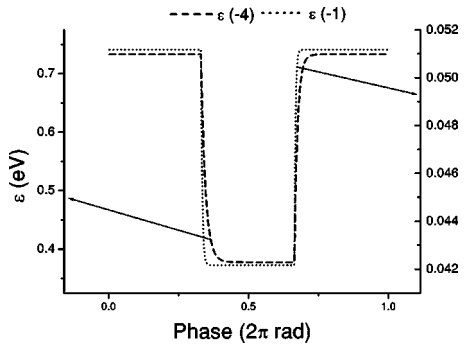

FIG. 1. Temporal relaxation of ε to step-function changes in the electric field ($E/n_0=0.5$ Td for $2\pi/3\leqslant\omega t\leqslant 4\pi/3$ and $E/n_0=1$ Td otherwise) for the hard sphere model. Values in the parentheses denote the power of 10 for the ratio m/m_0. ($\omega/n_0=10^{-18}$ rad m^3 s^{-1}.)

our discussion to electrons, but in Sec. III A 3 we demonstrate the extension to heavier ions.

1. Traditional prescriptions

Traditional descriptions of electron swarms in ac electric fields generally focus on the relation between the field frequency and the various collision frequencies governing the relaxation of these properties, e.g., within the confines of the two-term approximation, the isotropic component is governed by the energy transfer collision frequency, while the anisotropic (or vector) component is generally governed by the momentum transfer collision frequency [12,20]. These collision frequencies give a measure of the ability of the various properties to relax before the field changes. Comparison of these collision frequencies with the frequency of the field then gives rise to four frequency domains, each characterized by distinct modulation and phase lag properties in the temporal profiles. These regimes are distinct for electrons (or light ion swarms) by virtue of the disparity in the two governing collision frequencies.

For electrons, one assumes that an increase in the applied frequency generally results in a reduction in the amplitude of oscillation of the property and an increase in the phase delay of that properties profile with respect to the field [20]. This generalization has been further propagated through the use of the semiempirical ''effective field theories'' for electrons [6,17,20,32,33]. Recent numerical techniques and improved analytical treatments have shown that this generalization is not globally valid [e.g., (i) there can be an increase in the amplitude of the velocity profile [12,26], (ii) diffusion has a decidedly anomalous nature [16,25]]. In general, the ac electron transport properties display a more detailed structure than the sinusoidal profiles generally predicted in the traditional harmonic analyses [5,12,20].

2. Use of relaxation profiles

The detailed structure in the temporal profile of a transport property in an ac electric field can *best* be understood by appealing to the relaxation profile of that transport property in response to step changes in the field [29,46]: *One must consider not only the ability of the transport property to relax on a time scale governed by the frequency of the field but also the implications associated with an inability to relax*.

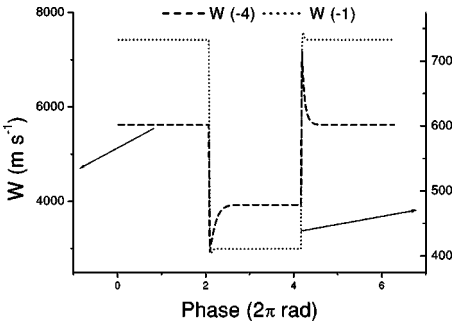

FIG. 2. Temporal relaxation of W to step-function changes in the electric field ($E/n_0=0.5$ Td for $2\pi/3\leqslant\omega t\leqslant 4\pi/3$ and $E/n_0=1$ Td otherwise) for the hard sphere model. Values in the parentheses denote the power of 10 for the ratio m/m_0. ($\omega/n_0=10^{-18}$ rad m^3 s^{-1}.)

The relaxation profiles associated with a step-function change in the electric field for the various transport properties are displayed in Figs. 1–5 for two different mass ratios $m/m_0=10^{-4}$ and 0.1, respectively, though we focus on the former in this section. For a given mass ratio, these profiles are dependent on the field magnitude, the change in the magnitude and sign of the field, and are further influenced by the *implicit* time dependence of the collision rates upon the time variation of the average energy of the swarm. The relaxation times for this constant cross-section model are effectively inversely proportional to the square root of the average energy. Thus, for a lower field (or equivalently energy), the relaxation times increase. It must be emphasized that the relaxation profiles are not necessarily monotonic (see, e.g., Figs. 2 and 5).

Using profiles in Figs. 1–5, one can now consider and understand the implications of the inability of a transport property to relax. The subsequent implications for ac electric fields can be further emphasized by approximating the ac electric field as a series of such step functions. In Fig. 6, the mean energy of the electrons is considered at various field frequencies for this step-function approximation to the ac

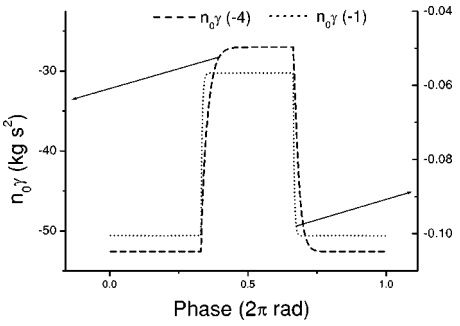

FIG. 3. Temporal relaxation of $n_0\gamma$ to step-function changes in the electric field ($E/n_0=0.5$ Td for $2\pi/3\leqslant\omega t\leqslant 4\pi/3$ and $E/n_0=1$ Td otherwise) for the hard sphere model. Values in the parentheses denote the power of 10 for the ratio m/m_0. ($\omega/n_0=10^{-18}$ rad m^3 s^{-1}.)

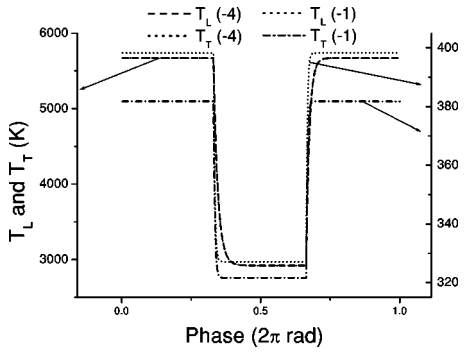

FIG. 4. Temporal relaxation of T_L and T_T to step-function changes in the electric field ($E/n_0=0.5$ Td for $2\pi/3\leqslant\omega t\leqslant 4\pi/3$ and $E/n_0=1$ Td otherwise) for the hard sphere model. Values in the parentheses denote the power of 10 for the ratio m/m_0. ($\omega/n_0=10^{-18}$ rad m^3 s^{-1}.) It should be highlighted that for $m/m_0=10^{-4}$ there is essentially no visible difference between $T_L(t)$ and $T_T(t)$.

field. The time step available for relaxation is inversely proportional to the field frequency. At low frequencies (viz., $\omega/n_0=10^{-26}$ rad m^3 s^{-1}), the time steps are sufficiently long to ensure there is full relaxation before the field changes, and the profiles are fully modulated and in phase with field. As we increase the frequency (or equivalently decrease the duration of each time step), in the low and decreasing field magnitude section of the cycle, the relaxation time for this property is sufficiently long that it cannot fully relax before the field changes and the value at the end of the step is greater than the equivalent ''steady state'' value. When the field changes sign and is increasing in magnitude, the initial value for a given step is actually greater than the equivalent steady state value for that value of the field in that step function. Hence, the energy falls even though the field magnitude is rising. The converse applies when the field magnitude passes its maximum. Herein lies the origin of the reduction in the modulation amplitude and increase in the phase lag with increasing frequency. It should be emphasized that this generalization applies only to other *monotonically* relaxing transport properties, e.g., D_T, T_T, T_L, and γ.

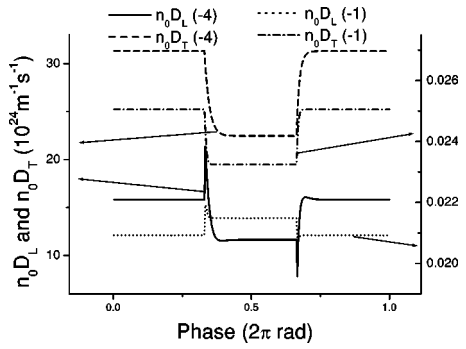

FIG. 5. Temporal relaxation of n_0D_L and n_0D_T to step-function changes in the electric field ($E/n_0=0.5$ Td for $2\pi/3\leqslant\omega t\leqslant 4\pi/3$ and $E/n_0=1$ Td otherwise) for the hard sphere model. Values in the parentheses denote the power of 10 for the ratio m/m_0. ($\omega/n_0=10^{-18}$ rad m^3 s^{-1}.)

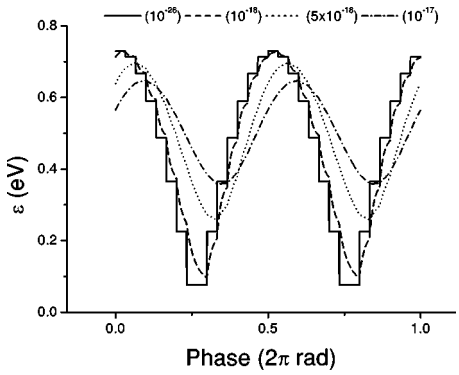

FIG. 6. The temporal variation of ε for the hard sphere model (cold gas) for a step-function approximation to the field at various applied reduced angular frequencies in parentheses (units of ω/n_0, rad m^3 s^{-1}).

Nonmonotonicity in the relaxation profiles gives rise to further interesting phenomena in ac electric fields. The nonmonotonicity in the relaxation profiles arises from the existence of two or more time constants associated with the constitutive influences on that property. Let us consider, for example, the $m/m_0=10^{-4}$ drift profile in Fig. 2 and apply the arguments used in the step-function approximation to the field for the mean energy. If the field frequency is increased to a value where the drift velocity can no longer relax sufficiently before the field changes, then we have the situation where the property has ''overshot'' its steady state value and thus at the end of a given step the value may be increased/decreased over its steady state value if the field magnitude is increasing/decreasing. This is the origin of the nonsinusoidal behavior and the maximal property of the amplitude with frequency [26] in the ac electron drift velocity profiles. It should be emphasized that one need also consider the response (or equivalently the relaxation profile) of the transport property to a change in the field direction to fully understand the ac profiles [25]. For an exhaustive description of this approach to understanding the temporal profiles in ac electric fields, the reader is referred to Ref. [46].

3. Extension to heavier ions

We have outlined above a general ''recipe'' by which all charged-particle phenomena in ac electric fields can be understood. The task of understanding the influence of the mass ratio on the ac temporal profiles then reduces to understanding its influence on the relaxation profiles as shown in Figs. 1– 5. We will return to such arguments and the $m/m_0=0.1$ relaxation profiles in Figs. 1– 5 throughout the course of the following discussions.

B. Drift velocity

The drift velocity profiles for various mass ratios and field frequencies are displayed in Fig. 7. For an increasing mass ratio at a given field frequency we observe (1) a reduction in the rms drift velocity, (2) an increase in the phase delay, and (3) a reduction in the nonsinusoidal behavior of the profiles. We also note that a reduction in the maximal property of the

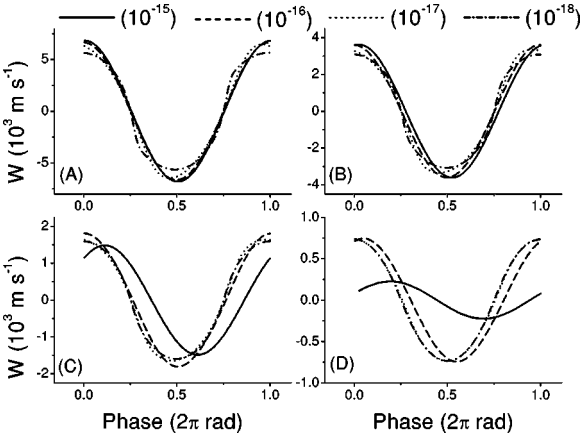

FIG. 7. Temporal profiles of W for various reduced angular frequencies ω/n_0 in parentheses (rad m^3 s^{-1}) and mass ratios: (A) $m/m_0=10^{-4}$; (B) $m/m_0=10^{-3}$; (C) $m/m_0=10^{-2}$; (D) $m/m_0=10^{-1}$.

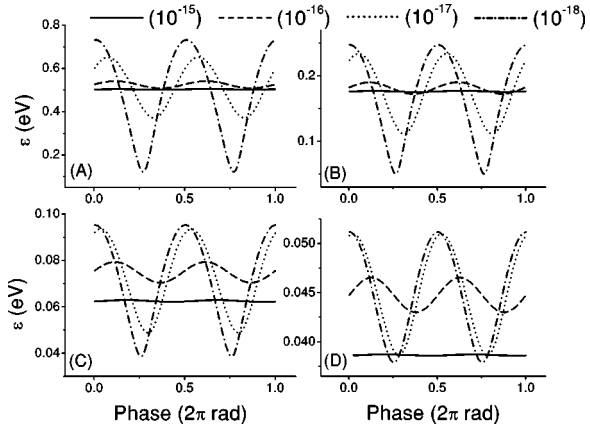

FIG. 8. Temporal profiles of ε for various reduced angular frequencies ω/n_0 in parentheses (rad m^3 s^{-1}) and mass ratios: (A) $m/m_0=10^{-4}$; (B) $m/m_0=10^{-3}$; (C) $m/m_0=10^{-2}$; (D) $m/m_0=10^{-1}$.

amplitude of oscillation with frequency as the mass ratio is increased (higher frequencies have been calculated but are not shown here).

As discussed in Sec. III A, the maximal property and nonsinusoidal behavior are associated with an overshoot in the relaxation profile for the drift velocity. For an increasing mass ratio we observe from Fig. 2 that this ''overshoot'' is reduced and the reduction of the maximal property with frequency and transition toward sinusoidal profiles with increasing mass ratio then follows using the arguments of Sec. III A. The overshoot in the relaxation profiles arises from the difference in the relaxation times of the constitutive influences (viz., the initial response of W to changes in the field is governed by ν_m while the long term response is governed by ν_e—an implicit effect of the energy variation in the collision frequency). For low mass ratios there is a large separation in the relaxation times of the constituent influences on W. As m/m_0 increases this separation reduces and consequently so too does the overshoot.

Physically, increasing m/m_0 acts to reduce the randomization of swarm-particle velocities caused by elastic collisions and the ability of the swarm to respond to changes in the field magnitude and direction is subsequently reduced. This is reflected in the increase in the time required for the swarm to relax to its overshot value (i.e., the relaxation time of the initial transient) in Fig. 2. The increase in the phase lag with respect to the field with increasing m/m_0 then follows.

C. Mean energy

The mean energy profiles for various mass ratios are displayed at various frequencies in Fig. 8. We note for an increase in the mass ratio at a given frequency, (1) a decrease in the cycle-averaged value of the mean energy, (2) a decrease in the amplitude of modulation, and (3) a decrease in the phase delay of the profile with respect to the field. In addition, for a given mass ratio, a maximal property with frequency in the cycle-averaged value is observed. The origin of this property for electrons is well understood and has been discussed analytically elsewhere [26].

The reduction of the cycle-averaged value with m/m_0 is a consequence of two factors.

(1) The enhanced energy transferred per elastic collision as m/m_0 increases enables the ''steady state'' to be reached at lower energies.

(2) The increase in the phase lag of W with increasing m/m_0 results in a reduction in the ability of the electric field to input power into the swarm.

The phase lag properties of ε follow directly from the associated relaxation profiles in Fig. 1. Here, with an increasing mass ratio we observe a reduction in the relaxation time for the profile. Although the implicit effect of a decreasing ε is to reduce the collision frequency (and hence act to increase the relaxation time), the increased energy transfer per elastic collision enables the swarm to quickly dissipate excess energy (for a falling field) or equivalently reach its steady state (for an increasing field) and this appears to be the dominant effect.

D. Diffusion

The influence of the ion-neutral mass ratio on the temporal profiles of the longitudinal and transverse diffusion coefficients in ac electric fields of differing frequencies is displayed in Fig. 9. Before we begin a detailed discussion of the phenomenon of anomalous anisotropic diffusion, we will briefly review the origin of anisotropic diffusion in dc electric fields. The *two* sources of anisotropy are (1) thermal anisotropy, dispersion of charged particles associated with random motions is *different* in the directions parallel and perpendicular to $\boldsymbol{E}$; (2) differential velocity effect, the spatial variation of local average velocities through the swarm combined with an energy dependent collision frequency act to influence the spread of the swarm parallel to field [25,47].

In review, if we consider a pulse of swarm particles drifting and diffusing under the influence of a dc electric field, then those at the front of the swarm will have a higher energy than those at the trailing edge. (There is no spatial variation

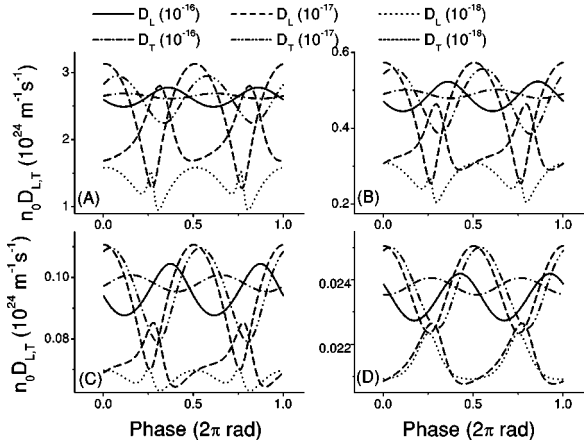

FIG. 9. Temporal profiles of n_0D_L and n_0D_T for various reduced angular frequencies ω/n_0 in parentheses (rad m^3 s^{-1}) and mass ratios: (A) $m/m_0 = 10^{-4}$; (B) $m/m_0=10^{-3}$; (C) $m/m_0=10^{-2}$; (D) $m/m_0=10^{-1}$.

in the mean energy transversing the field.) If the collision frequency increases with energy ($\nu_m'>0$) then those at the front of the swarm will have a smaller instantaneous drift than those at the tail. This ''differential velocity effect'' will act to retard the expansion of the swarm in the direction of the electric field. Of course, random particle motions (thermal component of the diffusion tensor) always act to spread the swarm, though the anisotropic nature of the temperature tensor will influence the rate of spreading in the different directions. The differential velocity effect will thus act to slow the rate of spreading parallel to the field as compared with the rate perpendicular to the field. These combined effects can be summarized in the following empirical relations for dc electric fields (generalized Einstein relation—see, e.g., [34]):

$$\frac{D_L}{D_T}=\frac{T_L}{T_T}\frac{\partial \ln W}{\partial \ln E}, \tag{19}$$

$$=\frac{T_L}{T_T}+\frac{\mu \nu_m' \gamma W}{kT_T}. \tag{20}$$

For electrons in a cold gas with a hard sphere interaction model (as considered here), a ratio $D_L/D_T\approx 0.5$ (actual value is 0.492) is predicted. The factor $\partial \ln W/\partial \ln E$ is fixed for this model and hence the departure of D_L/D_T from ≈ 0.5 in a cold gas in a dc field is indicative of anisotropy in the temperature tensor.

1. Anomalous anisotropic diffusion in ac electric fields—electrons

In previous work [25,46] we have studied the anomalous nature of electron diffusion in ac electric fields over a wide range of field frequencies. For the present discussion it will suffice to reference the $m/m_0=10^{-4}$ profiles in Fig. 9. There are some striking effects in the diffusion coefficients:

(1) At low frequencies we observe the evolution of a spike in the low-field phase of the cycle. As the frequency increases the height and temporal extent of the spike is increased until it becomes the dominant feature in the temporal profile of D_L;

(2) There exist phases in the field where $D_L/D_T\neq 0.5$ and indeed cases where $D_L>D_T$ in contrast to the dc steady state case. The fraction of the field where the latter relation holds increases with increasing frequency until they are antiphase. Instantaneously, for a given frequency, diffusion is isotropic four times per cycle;

(3) In a cycle averaged sense, D_L/D_T increases from 0.5 at low frequencies to 1 at high frequencies.

The origin of anomalous nature of the anisotropic diffusion has been discussed elsewhere [16,25,28,46]. The spike in the D_L profile is a signature not only of a nonmonotonically relaxing transport coefficient, but one in which the initial transient response is opposite to the long term response as shown in Fig. 5 (e.g., the response is through a higher value before relaxing to a value lower than the initial value). To further emphasize this, we again consider the ac electric field as a series of step functions as shown in Fig. 10. The spike appears in the low-field (low-energy) phase of the cycle where the relaxation time is longer. As the field frequency increases the phases of the field where full relaxation is prevented increases and the ''spike'' component then dominates the profile.

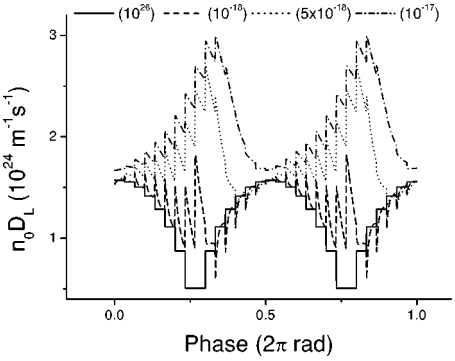

FIG. 10. The temporal variation of n_0D_L for the hard sphere model (cold gas) for a step-function approximation to the field at various applied reduced angular frequencies in parentheses.

It is interesting in this case to note that the phases of instantaneous isotropic diffusion correspond to phases of field where drift velocity is zero and the spatial variation of the mean energy (γ) is zero. The phases of the field where $D_L>D_T$ correspond to phases where $\gamma(t)W(t)>0$. Here the spatial variation in the swarm cannot respond to a change in the field direction as quickly as the drift velocity. If one considers Eq. (20) to apply instantaneously, one can see in these phases that the differential velocity effect now acts to enhance longitudinal diffusion [25,46].

For ion swarms the situation is further complicated by the presence of an anisotropic temperature tensor and the modification of relaxation times for the various constituents. To attempt to understand the influence of the mass ratio on the phenomenon of anomalous anisotropic diffusion in ac electric fields we must, therefore, sample the temporal variation of the constituent components.

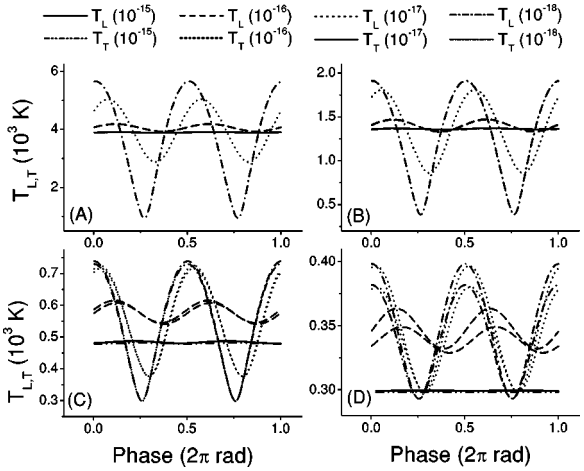

FIG. 11. Temporal profiles of T_L and T_T for various reduced angular frequencies ω/n_0 in parentheses (rad m^3 s^{-1}) and mass ratios: (A) $m/m_0=10^{-4}$; (B) $m/m_0=10^{-3}$; (C) $m/m_0=10^{-2}$; (D) $m/m_0=10^{-1}$.

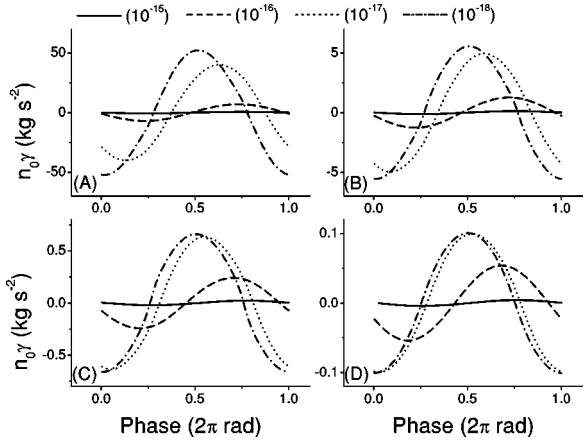

FIG. 12. Temporal profiles of $n_0\gamma$ for various reduced angular frequencies ω/n_0 in parentheses (rad m^3 s^{-1}) and mass ratios: (A) $m/m_0=10^{-4}$; (B) $m/m_0=10^{-3}$; (C) $m/m_0=10^{-2}$; (D) $m/m_0=10^{-1}$.

2. Temperature tensor

In dc swarms it is well known that an increase in the mass ratio results in increased anisotropy in the temperature tensor—the longitudinal component being greater than the transverse [34]. Equivalently, the velocity distribution function is elongated in the direction of the electric field force. The origin is primarily a result of the increased energy transfer per elastic collision that reduces the energy available transverse to the field post collision.

In Fig. 11 we display both the longitudinal and transverse temperature components as a function of the mass ratio and field frequency. In accordance with dc results, anisotropy of the temperature tensor develops as the mass ratio increases, independently of the field frequency. More specifically, at a given frequency we observe for an increase in the mass ratio, over the range of ω/n_0 and m/m_0 considered:

(1) A reduction in the cycle-averaged values $\overline{T_L}$ and $\overline{T_T}$, the inequality $\overline{T_L}\geqslant\overline{T_T}$ being satisfied at all frequencies;

(2) A reduction in the modulation amplitude of both components, with the modulation of $T_L\geqslant T_T$;

(3) An enhancement of the phase lag of T_T with respect to T_L.

Further analytic study is required to isolate the disparity in the relaxation times and associated phase lags in the ac profiles. It is interesting to note that the T_L and T_T profiles for $m/m_0=10^{-1}$ are closest at the phase of the field where W passes through zero, but are never equal for this mass ratio. This is indicative of a property whose controlling influences are convoluted rather than multiplicative, by virtue of timescales that are not too disparate.

3. Gradient energy parameter

The average energy of the swarm in a dc electric field is known to increase in the direction of the drift velocity—the charged particles at the front of the swarm have on an average fallen through a greater potential and hence on the average are more energetic than those at the tail. From Eq. (14) it then follows that this property is reflected in a negative value of γ. The magnitude of this property indicates the degree of spatial variation in the average energy through the swarm.

For ac electric fields, we note from Fig. 12 that for an increasing mass ratio, (1) the rms value decreases for a given frequency and (2) the phase lag with respect to the field decreases for a given frequency. Also, we note for a fixed mass ratio and increasing field frequency, (1) the rms value decreases and (2) an increase in the phase lag with respect to the field—for high frequencies; the phase lag appears to approach a value of π, independent of the mass ratio. Arguments used to explain these ac profiles from the associated relaxation profiles for this property are equivalent to those for ε. The origin of the reduction in the relaxation time with m/m_0, is the increased energy dissipated per elastic collision.

4. Diffusion in ac ion swarms

Before considering the detailed structure of the temporal profiles in ac fields, we should highlight an important point concerning the variation of the diffusion coefficients with an increasing mass ratio in a dc electric field (viz., the steady-state values in the relaxation profiles in Fig. 5). We note that (1) as m/m_0 increases, D_L changes from a monotonically increasing to monotonically decreasing function of E/n_0, and (2) D_T is a monotonically increasing function of E/n_0 for all m/m_0 considered. The first property results from the increasing relative contribution of the thermal motion of the background gas to the swarm properties as m/m_0 is increased for the field range considered—the swarm approaches thermal equilibrium with the neutrals and diffusion approaches isotropy. For background gas temperature of 0 K this property is no longer present.

The structure of the profiles for the electrons and those up to and including $m/m_0=10^{-2}$ in Fig. 9 are qualitatively equivalent and we would expect our arguments used in Sec. III D 1 to carry over to these mass ratios. For a mass ratio of 10^{-1}, however, we note (aside from the different quasi-dc behavior) that (1) the absence of a spike in the D_L profile in the low-energy phase at low frequencies and (2) the phases

of the field where $D_L > D_T$ *do not* correspond to those where $W\gamma > 0$. The absence of the spike can be seen directly from the relaxation profiles in Fig. 5: In contrast to other mass ratios, for $m/m_0 = 10^{-1}$ the initial and long term responses to a change in the field are in the *same* direction. As for the anomalous region, given $T_L \geqslant T_T$ over all phases of the field for this mass ratio, if one instantaneously applied the relation 20, one might expect the region where $D_L > D_T$ to subsume the criterion for smaller mass ratios ($W\gamma > 0$). In contrast to the smaller mass ratios, however, there does not occur the same separation of relaxation time scales of the constituent influences for a mass ratio of $m/m_0 = 10^{-1}$. The influence of the different physical mechanisms are now convoluted and physical understanding of the anomalous region is no longer obvious.

IV. CONCLUDING REMARKS

In summary, we have presented an investigation of the influence of the charged particle to neutral particle mass ratio on the transport coefficients of swarms in an ac electric field over a wide range of frequencies. The full time- and space-dependent Boltzmann equation (with the original Boltzmann collision operator) was solved in the time-dependent hydrodynamic regime combining techniques developed for ac electron swarms [25,27,29] with the machinery for dc ion swarms [39,42]. The technique is valid for arbitrary field frequencies and avoids the need to consider limiting mass ratio cases with various approximate collision operators.

The technique becomes increasingly inefficient as the mass ratio approaches unity. The calculation of the collision matrix for a given T_b is very computationally expensive in this limit and is inadequate for the consideration of nonperturbative field strengths. One technique that shows particular promise for this regime is the bi-Maxwellian treatment [48], where the calculation of the collision matrices at two ''appropriate'' T_b only are required, and the appropriate weightings are then used to account for time-variation effects.

We introduced a scheme to understand the temporal profiles of transport properties in ac electric fields through studies of the relaxation profiles of the various properties. This scheme enabled us to understand the removal of the spike in the D_L profile as the mass ratio is increased as well as the other mass ratio related effects on the modulation and phase relations of the various transport properties. The study points to the need for an analytic study of ion swarms in ac electric fields to fully comprehend some of the detailed modulation and phase lag relations (viz., an extension of the work of Robson *et al.* [28] to arbitrary mass ratios).

ACKNOWLEDGMENTS

The author gratefully acknowledges (i) discussions with Dr. Robert Robson and Dr. Kevin Ness, and (ii) the financial support of (a) Australian Academy of Science and the IREX scheme, and (b) JCU Research and International Division.

[1] M.A. Liebermann and A.J. Lichtenberg, *Principles of Plasma Discharges and Materials Processing* (Wiley, New York, 1994).
[2] K. Ness and R.E. Robson, Phys. Rev. A **39**, 6596 (1989).
[3] T. Makabe, *Gaseous Electronics and its Applications* (KTS Scientific, Tokyo, 1991).
[4] T. Holstein, Phys. Rev. **70**, 367 (1946).
[5] H. Margeneau and L.M. Hartman, Phys. Rev. **73**, 309 (1948).
[6] A.D. MacDonald and S.C. Brown, Phys. Rev. **75**, 441 (1949).
[7] J. Wilhelm and R. Winkler, J. Phys. Colloq. **40**, C7 (1979).
[8] R. Winkler, H. Deutsch, J. Wilhelm, and C. Wilke, Beitr. Plasmaphys. **24**, 284 (1984).
[9] D. Loffhagen and R. Winkler, J. Phys. D **29**, 618 (1996).
[10] D. Loffhagen and R. Winkler, Plasma Sources Sci. Technol. **5**, 710 (1996).
[11] D. Loffhagen, G.L. Braglia, and R. Winkler, Contrib. Plasma Phys. **38**, 527 (1998).
[12] T. Makabe and N. Goto, J. Phys. D **21**, 887 (1988).
[13] N. Goto and T. Makabe, J. Phys. D **23**, 686 (1990).
[14] K. Maeda and T. Makabe, Jpn. J. Appl. Phys., Part 1 **33**, 4173 (1994).
[15] K. Maeda and T. Makabe, Phys. Scr. **T53**, 61 (1994).
[16] K. Maeda, T. Makabe, N. Nakano, S. Bzenic, and Z.L. Petrovic, Phys. Rev. E **55**, 5901 (1997).
[17] C.M. Ferreira and J. Loureiro, J. Phys. D **17**, 1175 (1984).
[18] C.M. Ferreira and J. Loureiro, J. Phys. D **22**, 76 (1989).
[19] C.M. Ferreira, L.L. Alves, M. Pinheiro, and A.B. Sa, IEEE Trans. Plasma Sci. **19**, 229 (1991).
[20] J. Loureiro, Phys. Rev. E **47**, 1262 (1993).
[21] Z.L. Petrovic, J.V. Jovanovic, Z.M. Raspopovic, S.A. Bzenic, and S. Vrhovac, Aust. J. Phys. **50**, 591 (1997).
[22] Z.M. Raspopovic, S. Sakadzic, S.A. Bzenic, and Z.L. Petrovic, IEEE Trans. Plasma Sci. **27**, 1241 (1999).
[23] S. Bzenic, Z. Raspopovic, S. Sakadvic, and Z.L. Petrovic, IEEE Trans. Plasma Sci. **27**, 78 (1999).
[24] S. Bzenic, Z.L. Petrovic, Z. Raspopovic, and T. Makabe, Jpn. J. Appl. Phys. **38**, 6077 (1999).
[25] R.D. White, R.E. Robson, and K.F. Ness, Aust. J. Phys. **48**, 925 (1995).
[26] R.E. Robson, K. Maeda, T. Makabe, and R.D. White, Aust. J. Phys. **48**, 335 (1995).
[27] R.D. White, R.E. Robson, and K.F. Ness, J. Vac. Sci. Technol. A **16**, 316 (1998).
[28] R.E. Robson, R.D. White, and T. Makabe, Ann. Phys. (Leipzig) **261**, 74 (1997).
[29] R.D. White, R.E. Robson, and K.F. Ness, Phys. Rev. E **60**, 7457 (1999).
[30] L. Boltzmann, Wein. Ber. **66**, 275 (1872).
[31] B.I. Davydov, Phys. Z. Sowjetunion **8**, 59 (1935).
[32] U. Korsthagen, Plasma Sources Sci. Technol. **26**, 1230 (1993).
[33] U. Korsthagen, Plasma Sources Sci. Technol. **4**, 172 (1995).
[34] E.A. Mason and E. W. McDaniel, *Transport Properties of Ions in Gases* (Wiley, New York, 1988).
[35] R.E. Robson and T. Makabe, Aust. J. Phys. **47**, 305 (1994).

[36] K. Kumar, Aust. J. Phys. **48**, 365 (1995).
[37] H. Sugawara, H. Tagashira, and Y. Sakai, J. Phys. D **29**, 1168 (1996).
[38] L.A. Viehland, E.A. Mason, and J.H. Whealton, J. Chem. Phys. **62**, 4715 (1975).
[39] K.F. Ness and R.E. Robson, Transp. Theory Stat. Phys. **14**, 257 (1985).
[40] K. Kumar, Aust. J. Phys. **20**, 205 (1967).
[41] K. Kumar, Ann. Phys. (N.Y.) **37**, 113 (1967).
[42] S.L. Lin, R.E. Robson, and E.A. Mason, J. Chem. Phys. **71**, 3483 (1979).
[43] K.F. Ness and R.E. Robson, Phys. Rev. A **34**, 2185 (1986).
[44] R.E. Robson and K.F. Ness, Phys. Rev. A **33** (3), 2068 (1986).
[45] K. Kumar, H.R. Skullerud, and R.E. Robson, Aust. J. Phys. **86**, 845 (1980).
[46] R.D.White, Ph.D. thesis, James Cook University, Department of Computer Science, Mathematics and Physics, 1996.
[47] H.R. Skullerud, J. Phys. B **2**, 696 (1969).
[48] K.F. Ness and L.A. Viehland, Chem. Phys. **148**, 225 (1990).